Hydrogeol J (2016) 24:1921–1937
DOI 10.1007/s10040-016-1454-3

PAPER

Spatial and temporal constraints on regional-scale groundwater flow in the Pampa del Tamarugal Basin, Atacama Desert, Chile

Richard S. Jayne[1,3] · **Ryan M. Pollyea**[1,3] · **Justin P. Dodd**[1] · **Elizabeth J. Olson**[1] · **Susan K. Swanson**[2]

Received: 21 February 2016 / Accepted: 18 July 2016 / Published online: 6 August 2016

Abstract Aquifers within the Pampa del Tamarugal Basin (Atacama Desert, northern Chile) are the sole source of water for the coastal city of Iquique and the economically important mining industry. Despite this, the regional groundwater system remains poorly understood. Although it is widely accepted that aquifer recharge originates as precipitation in the Altiplano and Andean Cordillera to the east, there remains debate on whether recharge is driven primarily by near-surface groundwater flow in response to periodic flood events or by basal groundwater flux through deep-seated basin fractures. In addressing this debate, the present study quantifies spatial and temporal variability in regional-scale groundwater flow paths at 20.5°S latitude by combining a two-dimensional model of groundwater and heat flow with field observations and $\delta^{18}O$ isotope values in surface water and groundwater. Results suggest that both previously proposed aquifer recharge mechanisms are likely influencing aquifers within the Pampa del Tamarugal Basin; however, each mechanism is operating on different spatial and temporal scales. Storm-driven flood events in the Altiplano readily transmit groundwater to the eastern Pampa del Tamarugal Basin through near-surface groundwater flow on short time scales, e.g., 10^0–10^1 years, but these effects are likely isolated to aquifers in the eastern third of the basin. In addition, this study illustrates a physical mechanism for groundwater originating in the eastern highlands to recharge aquifers and salars in the western Pampa del Tamarugal Basin over timescales of 10^4–10^5 years.

Keywords Arid regions · Groundwater flow · Numerical modeling · Chile

Electronic supplementary material The online version of this article (doi:10.1007/s10040-016-1454-3) contains supplementary material, which is available to authorized users.

✉ Ryan M. Pollyea
rpollyea@vt.edu

[1] Department of Geology and Environmental Geosciences, Northern Illinois University, DeKalb, IL 60115, USA

[2] Department of Geology, Beloit College, Beloit, WI 53511, USA

[3] Department of Geosciences, Virginia Polytechnic Institute and State University, Blacksburg, VA 24060, USA

Introduction

The Atacama Desert in northern Chile is among the driest regions on Earth, receiving less than 5 mm of precipitation per year (Clarke 2006). This extreme climate is of particular interest for groundwater investigations because arid regions are highly sensitive to subtle variations in climate (Amundson et al. 2012; Gayo et al. 2012; Nuñez et al. 2011; Rech et al. 2010; Hoke et al. 2004). Consequently, hydrogeological processes in the Atacama Desert may be a useful proxy for understanding the implications of expanding global aridity. The most economically important aquifer system in the Atacama Desert lies within the Pampa del Tamarugal (PdT) Basin, which is a broad, relatively flat basin bounded on the east by the Andean Altiplano and on the west by the Chilean Coastal Range (Fig. 1). Aquifers within the PdT Basin are the sole source of potable and industrial water for the cities of Iquique and Arica, and are the primary water supply for northern Chile's economically important mining industry (Fritz et al. 1981; Oyarzún and Oyarzún 2011).

Although there is little debate over the source (and to a lesser extent timing) of groundwater recharge from the Altiplano into the PdT, there remains uncertainty surrounding the mechanisms and magnitudes of this groundwater flux. Numerous investigators have studied regional hydrologic processes, with an emphasis on understanding groundwater flow

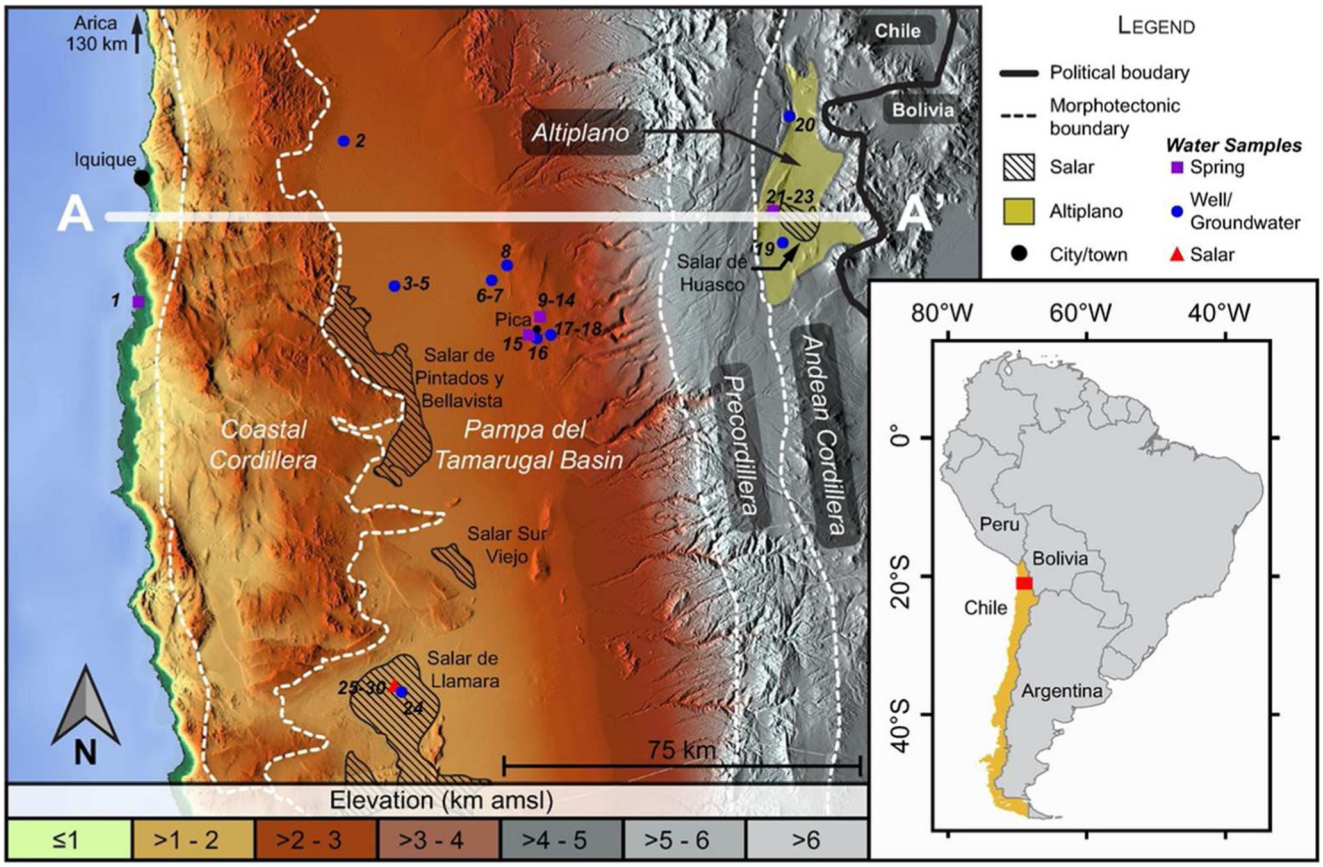

Fig. 1 Shaded relief map of the study area. Transect *A*–*A′* is the lateral extent of the numerical model domain, which is at ~20.5°S latitude and 158 km wide. The locations of water samples collected as part of this study (1–30) and sample type (i.e. spring, groundwater, salar) are noted on the map. See Table S1 of the electronic supplementary material (ESM) for detailed descriptions of sample locations

from the Andean Altiplano into the PdT basin. Oxygen and hydrogen isotope variation in surface and subsurface waters from the region suggest that groundwater discharging to springs and salars in the eastern PdT likely results from infiltration and gravity-driven fluid migration from the Altiplano (e.g. Fritz et al. 1981; Aravena et al. 1999). The prevalence of Pleistocene-aged (^{14}C-dated) wetland deposits at 2,500 m above mean sea level (amsl) in northern Chile suggests that the last major period for perennial stream discharge into the PdT Basin occurred ~ 18,000 years ago (Nester et al. 2007). Subsequent work by Gayo et al. 2012 reconstructed the late Pleistocene–Holocene climate record in the PdT by documenting regional scale variation in archeological sites, paleoecology, and carbon isotope variations in organic material to infer three climate-driven aquifer recharge (pluvial) periods in the PdT occurring at 17.6–14.2, 12.1–11.4, and 1.01–0.71 ka, and the authors suggest modern PdT aquifers receive little, if any, naturally occurring recharge.

Recent studies of the mechanisms and magnitudes of groundwater flux from the Altiplano to the PdT differ in their conclusions regarding the relative importance of deep versus shallow flow paths. Magaritz et al. 1990 combined the aquifer thermal profile and ^{14}C groundwater ages to present a conceptual model suggesting that meteoric water penetrates deep within the Cordillera before circulating upward into the PdT by topographic driving potential and thermal gradients through fault-controlled migration pathways (Fig. 2, black arrows). The Magaritz et al. 1990 conceptual model is a convincing observational argument for deep fluid circulation, and is in general agreement with mechanics governing topography-driven fluid flow (Tóth 1962, 1963); however, the mechanism is poorly constrained at the subbasin scale. In contrast, Houston 2002 used the hydrograph response from a major 2001 flooding event comprising an estimated 34 Mm^3 of overland flow to show that infiltrating precipitation from the Altiplano to the PdT is governed by shallow topography driven flow through alluvial fan systems (Fig. 2, white arrow). In addition, Houston 2002 constrained the magnitude of this basin recharge flux to be 200 L/s over a 4-year period following the flash flood, and argues that residual hydraulic head from these flood events may be sufficient to drive aquifer recharge across the lateral extent of the PdT Basin. As a result, this model suggests that alluvial fan drainage is likely the primary groundwater recharge mechanism within the basin because flood events of this type have a 4-year recurrence interval.

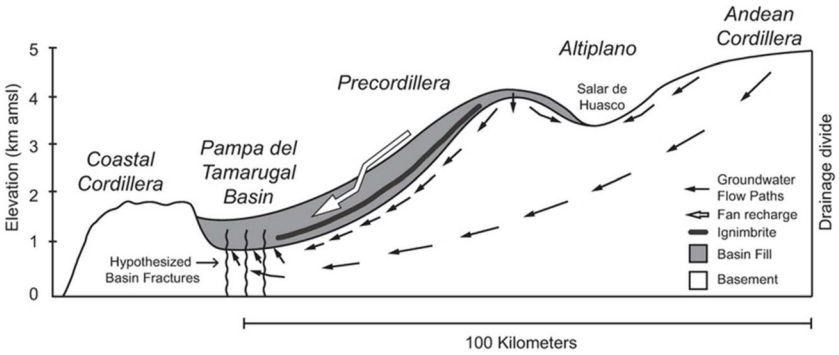

Fig. 2 Conceptual model of regional scale groundwater circulation from the Altiplano and Andean Cordillera to the Pampa del Tamarugal Basin. *Black arrows* illustrate the recharge mechanism by which deep, thermally driven groundwater enters the basin through deep-seated basin fractures (Magaritz et al. 1990). The *white arrow* illustrates the recharge mechanism by which periodic flood events in the Altiplano recharge the basin through surface infiltration and near-surface groundwater flow (Houston 2002). General schematic adapted from Magaritz et al. (1990)

The seemingly incompatible aquifer recharge mechanisms pose a significant challenge to groundwater resource management in the region—for example, the Houston (2002) recharge model has been adopted in the most recent conceptual model of PdT aquifer geometry (Rojas et al. 2010), as well as a basin-wide numerical model used to quantify future groundwater resources within the PdT Basin (Rojas and Dassargues 2007). In this latter model, the authors specify the Houston (2002) alluvial fan recharge model as a Neumann (fixed flux) boundary condition representative of alluvial fan recharge along the eastern extent of the model domain, while neglecting basal groundwater flux by imposing an adiabatic boundary (no fluid flux) across the bottom of the model domain. Although there is convincing evidence that groundwater enters the PdT aquifer through deep hydrothermal circulation (Houston 2002), the adiabatic basal boundary condition specified by Rojas and Dassargues (2007) is a reasonable choice because the magnitude and spatial distribution of this basal groundwater flux has not been constrained. To develop a quantitative conceptual model constraining the magnitude and spatial distribution of regional groundwater flux, as well as first-order estimates of groundwater residence time across the study area, this work combines a regional scale two-dimensional (2-D) numerical model of groundwater and heat flow with oxygen isotope ($\delta^{18}O$) measurements from groundwater and spring samples.

Study area

The study area is a 158 km west-to-east transect at ~20.5°S latitude that begins 4 km off the Pacific coast of Chile and extends east through PdT Basin to the Bolivian border (Fig. 1, A–A′). The elevation profile for transect A–A′ ranges from sea level at the Pacific coast to 4,900 m at the peak of the Andean Cordillera (Fig. 3). Transect A–A′ was selected due to its proximity to Iquique so that results may be of use for regional groundwater management.

Climate

The PdT Basin lies within the Atacama Desert, and covers an areal extent of ~105,000 km^2 in three South American countries, including portions of Bolivia, Chile, and Peru. This region is of scientific interest for both its natural mineral resources and its extreme, hyper-arid climate, which is characterized by less than 5 mm/yr of precipitation in most areas (Clarke 2006; Hartley et al. 2005; Houston 2002; Rojas and Dassargues 2007. The Atacama Desert is among the oldest deserts on the planet with some studies suggesting that the Atacama has been arid for the last 150 Ma (Hartley et al. 2005). Additionally, the Atacama Desert has been located at the same latitude since the late Jurassic, and there exists a fairly continuous sedimentary record of arid to semi-arid climate (Hartley et al. 2005; Houston 2005).

Although the regional climate has been generally stable, researchers have noted a drying period ~19–13 Ma BP (Alpers and Brimhall 1988; Rech et al. 2006; Sillitoe and McKee 1996). One hypothesis for this drying period is that during this time the western flank of the Andean Cordillera was approximately half of its present day elevation, and increasing elevation through the lower-middle Miocene resulted in an increasing rain shadow effect (Farías et al. 2005; Garizone et al. 2008; Gregory-Wodzicki 2000; Lamb and Hoke 1997). In contrast to this model, Garreaud et al. 2010 developed a climate model suggesting the Western Cordillera rain shadow has not contributed to the drying climate and the largest contributing factor is the appearance of the Hadley Cell ~25 Ma. The Hadley Cell creates a sub-tropical anticyclone hindering mid-latitude disturbances, which aid the Humboldt Current causing north winds to remain along the Chilean coast and assisting in the transport of cold water from higher latitudes (Garreaud et al. 2010). While the Coastal Cordillera, PdT Basin, and most of the Precordillera receive little to no rain, the Altiplano receives increasing precipitation with increasing elevation (Houston 2002; Magaritz et al. 1989).

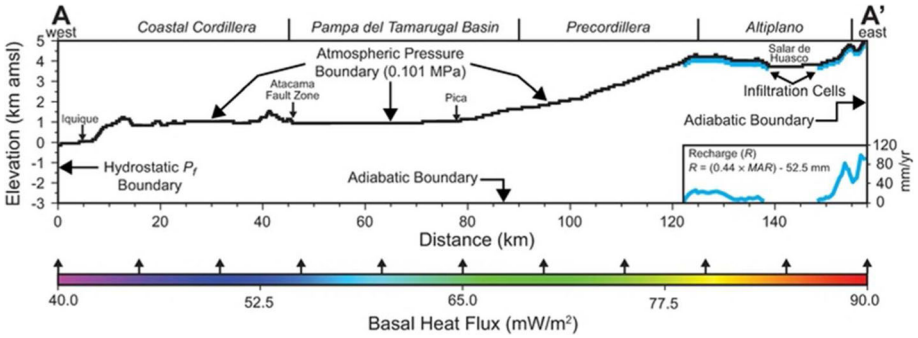

Fig. 3 Schematic illustration of model domain and boundary conditions for the numerical groundwater model across transect *A–A′*. The model domain is a 2-D Cartesian mesh with 80,018 grid cells specified with 100 m × 100 m × 100 m dimensions. Although the out-of-plane dimension is arbitrary for a 2-D model results, the surface area of each grid cell is required for the integral finite volume solution method used by TOUGH2-MP (Zhang et al. 2008). The *blue curve* illustrates elevation-dependent groundwater recharge (*R*) rate computed as a function of mean annual precipitation (*MAR*) by Eq. (1)

Geology

Transect A–A′ comprises the five regional morphotectonic features of northern Chile, which include the Coastal Cordillera, Pampa del Tamarugal (PdT) Basin, Precordillera, Altiplano, and Andean Cordillera (Fig. 1). The Coastal Cordillera is a N–S range trending parallel to the Peru-Chile trench with an average width of ~50 km and elevations as high as 3 km. The Coastal Cordillera is bound to the west by a Miocene age coastal escarpment with an elevation gain of up to 1 km (Hartley and Evenstar 2010). Within the study area, the Coastal Cordillera is comprised of Jurassic age volcanic arc remnants, including (1) the Caleta Ligate Formation, which is a ~600 m thick layer of volcaniclastic rocks, limestone, and basaltic andesites; (2) the Officina Viz Formation, which underlies the Caleta Ligate and is composed of basaltic andesite and andesitic lava piles with a minimum thickness of 1,500 m; and (3) the Pre-Cambrian granitic-gneissic basement rock, which underlies the Caleta and Officina Viz formations (Fig. 4). These volcanic formations extend offshore towards the Peru-Chile trench Kösters et al. (1997), and are now cross-cut by a series of extensional faults (Gregory-Wodzicki 2000; Hartley et al. 2000; Hartley and Evenstar 2010; Kramer et al. 2005). The eastern edge of the Coastal Cordillera is marked by the Atacama Fault Zone (AFZ), which is a N–S trending extensional and oblique strike-slip fault system (Dingman and Galli 1965; Nester 2008) that formed during the Late Jurassic and Early Cretaceous (Cembrano et al. 2005). The AFZ is considered to be a continental-scale feature, and has been mapped for ~1,000 km from Iquique (20°S) to La Serena (32°S). Loveless et al. 2005 describe the AFZ as having a very low permeability core ~3 m thick with a higher-permeability damage zone that extends ~100 m laterally to each side.

The PdT Basin is a forearc basin resulting from subduction of the Nazca plate beneath the South American plate. As is typical on the continental side of a subduction zone, an extensive graben complex developed and has since been filled with up to 1,700 m of non-marine, Oligocene to recent sediments (Dingman and Galli 1965; Houston 2002; Magaritz et al. 1989; Nester 2008; and Rojas and Dassargues 2007)

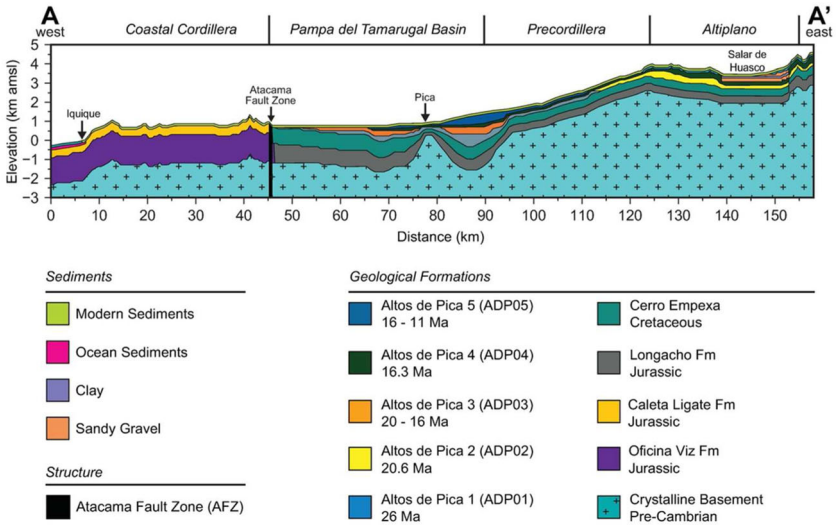

Fig. 4 Geological model of the study area transect illustrating the spatially distributed heterogeneity incorporated into the numerical groundwater model. Hydraulic and thermal properties for each geological formation are listed in Table 1

overlying the strongly folded Cenozoic basement rock (Nester 2008). The PdT Basin is the topographic low between the Coastal Cordillera and Precordillera with an average elevation of 1,000 m amsl. The non-marine sediments filling the basin at this latitude are collectively called the Altos de Pica Formation (AdP), which includes five members that alternate between sedimentary and volcanic deposits. AdP member 1 (AdP1) was deposited ~26 Ma BP and marks the beginning of uplift for the Altiplano. The AdP1 unit is a mix of fluvial and alluvial deposits comprising conglomerates interbedded with sandstones having an average aggregate thickness of 325 m (Dingman and Galli 1965; Nester 2008; Rojas and Dassargues 2007). AdP member 2 (AdP2) is a volcanic layer comprising rhyolitic tuff and andesitic ignimbrite that was deposited ~20.6 Ma BP when the volcanic arc was located in the present day Coastal Cordillera. The AdP member 3 (AdP3) is a sedimentary unit dating 20–16 Ma BP that was deposited when the Coastal Cordillera and Precordillera were present and provided the sedimentary fill for the basin. AdP3 has an average thickness of 175 m and consists primarily of medium- to coarse-grained sandstone, interbedded with conglomerates. AdP member 4 (AdP4) is the second volcanic deposit of rhyolitic tuff and andesitic ignimbrite deposited ~16.3 Ma BP. AdP4 is called the Huasco Ignimbrite because it outcrops near Salar de Huasco in the Altiplano (Fig. 4). AdP member 5 (AdP5) was deposited between 16 and 11 Ma BP, and consists of sandstone and conglomerates. JICA-DGA-PCI (1995) used borehole logs and pumping tests to obtain the aquifer parameters within the basin and found that AdP5 is the primary water-bearing unit for the PdT Aquifer. The sedimentary fill in this basin forms a symmetrical lens shape, thinning both to the east and west with the thickest part of the basin located ~15 km west of Pica (Fig. 4; Dingman and Galli 1965; Nester 2008; Rojas and Dassargues 2007). Underlying the sedimentary fill are the Cerro Empexa, Chacarilla, and Longacho formations, which are marine deposits consisting of mainly marine sandstones and shales that are interbedded with volcanic ignimbrites and tuffs (Dingman and Galli 1965; Houston 2002).

The Precordillera marks the eastern extent of the PdT Basin, where elevation increases sharply and AdP members 1, 3, and 5 start pinching out at ~2,000 m amsl. As a result, these units are no longer present by 3,200 m amsl, which results in ignimbrite units in direct contact with the Cenozoic marine deposits. The Precordillera crests at an average of 4,200 m amsl, and is bounded to the east by the high elevation plateau, which is known as the Altiplano (Victor et al. 2004).

The Altiplano and Andean Cordillera are the eastern-most features in the study area, and collectively form the modern day volcanic arc. The Altiplano has an average elevation of 4,000 m amsl, and is characterized by ignimbrite plateaus with north-trending ridges (Hartley and Evenstar 2010; Valero-Garcés et al. 1999). The Altiplano geology comprises (1) a shallow layer of alluvial and eolian deposits overlying approximately 1,200 m of AdP2 and AdP4 volcanic ignimbrite; (2) ~800 m of marine sandstone; and (3) the Pre-Cambrian granitic-gneissic basement rock (Dingman and Galli 1965; Horton et al. 2002; Houston 2002, 2005; Magaritz et al. 1989; Nester 2008). Along the western edge of the Altiplano is Salar de Huasco (Fig. 4), which is an important hydrological feature because it is one of the few areas in northern Chile where surface water is present. The geology underlying Salar de Huasco comprises a low-permeability clay layer from 10 to 50 m below ground surface, which is underlain by a high-permeability sandy gravel to ~300 m depth (Acosta and Custodio 2008). Salar de Huasco is recharged primarily by springs located along the basin walls and surface runoff in the high-elevation basin (Ave. 4,164 m amsl; 1,462 km^2; Uribe et al. 2015; Stoertz and Ericksen 1974). The Altiplano is bounded on the east by the Andean Cordillera, which comprises volcanic peaks, ignimbrite plateaus, and north-trending ridges with maximum elevation over 6,000 m amsl (Hartley and Evenstar 2010; Valero-Garcés et al. 1999).

Within the study area, salars are the predominant expression of surface water, and are present in the Altiplano and western PdT Basin (Fig. 1). Although the terms salar and playa are often used interchangeably, here salar is defined as a permanent body of groundwater-fed saline surface water with regional extent and several meters depth. In contrast, playas, which are also common in northern Chile, are shallow ephemeral saline pools that are scattered around mudflats within a central depression. Both salars and playas are characterized by salt crusts that can either be (1) actively evaporating brines and gypsum, or (2) a fossil salt crust that is similar in mineralogy to active salt crusts, but much thicker and no longer forming. Salars are commonly associated with playa deposits. For example, playa deposits in the Salar de Huasco have an areal extent of ~50 km^2, with ~2.5 km^2 of permanent surface water (Uribe et al. 2015; Dorador et al. 2010; Risacher et al. 2003). Salars are highly sensitive to changes in geologic and hydrologic conditions because the water budget outputs are driven primarily by evaporation (Stoertz and Ericksen 1974); however, industrial groundwater pumping has been implicated in rapidly shrinking salar footprints across much of the western PdT Basin (Oyarzún and Oyarzún 2011).

Materials and methods

Field sampling and analytical methods

A field campaign was completed in November 2014 to obtain 30 water samples from 23 accessible wells, springs, and salars across the study area transect. Samples were taken from both

the unconfined aquifers at unpumped wells (well depth ranged from 5 to 43 m), as well as at free-flowing surface water bodies. Transect A–A′ (Fig. 1) represents a generalized cross-section of the region; as such, sample locations within ~50 km have been projected onto the study area transect. The $\delta^{18}O$ values of water samples were measured at the Northern Illinois University stable isotope laboratories via CO_2 equilibration on a GasBench II coupled to a Thermo MAT253 isotope ratio mass spectrometer in continuous flow. $\delta^{18}O$ values are reported in VSMOW with an analytical precision of ±0.3 ‰.

Numerical modeling approach

As discussed in section 'Geology', the study area is a 158 km west-to-east transect at ~20.5°S latitude beginning 4 km off the Pacific coast and extending east to the Bolivian border (Fig. 1). In order to investigate the timing and flux magnitude of groundwater flow from the Altiplano into the Pampa del Tamarugal (PdT) Basin, a 2-D numerical model is developed to simulate regional-scale groundwater flow across the study area transect A–A′. The elevation profile for transect A–A′ is based on sampling the transect at 100 m intervals using Google Earth™ (Fig. 3), and the transect is discretized as a regular Cartesin grid comprising 80,018 total grid cells with 100 m × 100 m × 100 m dimensions. Although the out-of-plane grid cell dimension is arbitrary for a 2-D model, the simulation code used here (TOUGH2-MP, discussed later) is based on the integral finite volume method which is specified on the basis of 3-D grid cells; moreover, the horizontal surface area of each grid cell is needed for quantifying heat and mass flux across grid cell interfaces. The maximum thickness of the model domain is 8,000 m at the Chile-Bolivia border, which is ~4,000 m deeper than the mean elevation (1,100 m) of the PdT Basin. This domain thickness was chosen on the basis of Forster and Smith 1998, who show that groundwater flow regimes in mountainous regions can extend to depths comparable to regional topographic highs.

The regional geology described is modeled as a layered heterogeneous system (Fig. 4) with hydrogeologic and thermal properties listed in Table 1. Although the spatial distribution of transect geology is fairly well constrained (Dingman and Galli 1965), there is significant uncertainty surrounding thermal and hydraulic properties at the scale of interest for the present investigation. This parametric uncertainty is discussed in section 'Parameter selection and analysis'. In addition, there is uncertainty with respect to the orientation of the Atacama Fault Zone (AFZ). Loveless et al. (2005) suggests the AFZ comprises a 3-m core surrounded on each side by a damage zone extending ~100 m laterally; however, this work was based on 1-m IKONOS satellite imagery and provides little constraints on the fault orientation at depth. Mpodozis and Ramos (1989 and Victor et al. (2004) interpreted geophysical surveys of the region to suggest the AFZ is a vertical structure beyond 3 km depth; however, this work does not constrain the AFZ configuration at shallow depths. As a result, these two scales of inference are combined by projecting the AFZ as a vertical structure, which is discretized by three columns of grid cells. The center column represents the AFZ fault core and one adjacent column on each side represents the AFZ damage zone. In order to parameterize the AFZ, the damage zone permeability is taken as the arithmetic mean of literature permeability values for its cross-cutting formations, which are the Caleta Ligate, Oficina Viz, and the Pre-Cambrian Granitic-Gneissic basement rock. Permeability of the AFZ core is reduced two orders of magnitude on the basis of Evans et al. (1997), whose investigations of granitic and gneissic core samples from East Fork thrust faults in Wyoming suggest that damage zone permeability is 2–3 orders of magnitude higher than the fault core of the same parent lithology. Although the orientation and hydrogeologic parameters of the AFZ are poorly constrained, the effects on regional groundwater flow resulting from a low-permeability fault core and high-permeability damage zone are presumed to be suitable for the scale of this investigation. Moreover, the AFZ bounds the PdT to the west, which suggests that topographically driven groundwater flow from the eastern highlands will be minimally impacted by error associated with poor constraints on the AFZ. Nevertheless, caution is warranted in utilizing results of this modeling investigation for making inferences the west of the AFZ.

The code selection for this study is TOUGH2-MP (Zhang et al. 2008) compiled with EOS1 (Pruess et al. 1999), which is the equation of state module for simulating nonisothermal groundwater flow in porous and fractured geologic media. In this work, the combined effects of groundwater and heat flow are taken into account; however, fully saturated conditions are assumed to ground surface on the basis that the computational demands for simulating nonisothermal, unsaturated flow are unreasonably high and return negligible confidence gains at the scale of this investigation. A Dirichlet boundary condition is imposed at ground surface to maintain both atmospheric pressure (0.101 MPa) and mean annual ground surface temperature, the latter of which ranges between an maximum of 20.4 °C in the PdT basin to ~2.2 °C in the Andean Cordillera (Fig. 3). Similarly, a Dirichlet boundary is imposed at the western vertical boundary to maintain hydrostatic fluid pressure and a constant geothermal gradient (18 °C km^{-1}) in the far field of the model domain. Adiabatic pressure and temperature boundaries are defined at the eastern extent of the model domain on the basis that this position marks the South American drainage divide, which corresponds with the Chile-Bolivia border. In keeping with basin-scale groundwater flow models at similar scales (e.g., Pollyea et al. 2015; Ge and Garven 1989), the bottom hydrogeologic boundary is also defined as adiabatic (Fig. 3). In order to account for the regional geothermal heat flux, a Neumann type thermal

Table 1 Hydraulic and thermal properties for geologic materials in transect A–A′

Formation	Density (kg/m^3)	Porosity (-)	Permeability (m^2)	Thermal conductivity (W/m K)	Rock-grain specific heat (J/kg K)	Sources
Basement (k_h)	2,667	0.05	9.87×10^{-16}	2.55	790	a, b, c, d, e, f, g, m
Basement (k_v)	2,667	0.05	9.87×10^{-18}	2.55	790	a, b, c, d, e, f, g, m
Altos de Pica 1	2,500	0.25	5.36×10^{-13}	1.79	920	c, f, g
Altos de Pica 2	2,380	0.10	1.00×10^{-14}	3.10	1,040	a, b, d, e, g
Altos de Pica 3	2,500	0.25	5.30×10^{-12}	1.79	920	c, f, g
Altos de Pica 4	2,380	0.10	1.00×10^{-14}	3.10	1,040	a, b, d, e, g
Altos de Pica 5	2,500	0.25	5.30×10^{-13}	1.79	920	c, f, g
Caleta Ligate	2,980	0.17	1.05×10^{-17}	2.14	840	c, f, g, j
Oficina Viz	2,700	0.17	9.78×10^{-17}	2.40	1,050	a, b, d, e, f, i, j
Cerro Empaxa	2,650	0.15	5.26×10^{-14}	1.85	920	c, f, g
Longacho	2,650	0.05	9.87×10^{-16}	2.25	790	c, f, g
Sandy gravel	1,800	0.28	1.05×10^{-12}	1.79	920	c, f, k
Clay	1,470	0.45	1.05×10^{-18}	1.43	920	c, f, k
AFZ – damage zone	2,677	0.17	9.87×10^{-16}	2.55	790	c, f, g, j, l
AFZ – core	2,677	0.17	9.57×10^{-14}	2.55	790	c, f, g, j, l
Ocean sediments	2,500	0.25	1.00×10^{-12}	1.79	920	c, f, g
Modern sediments	2,500	0.30	5.30×10^{-12}	1.79	920	c, f, g

[a] Daly et al. (1966)
[b] Johnson and Olhoeft (1984)
[c] Fitts (2013)
[d] Brace (1980)
[e] Wang and Narasimhan (1985)
[f] Eppelbaum et al. (2014)
[g] Sharma (1997)
[h] Smyth and Sharp (2006)
[i] Bacon (1975)
[j] Farquharson et al. (2015)
[k] Fetter (2001)
[l] Evans et al. (1997)
[m] Huenges et al. (1997)

boundary condition is imposed across the bottom of the model domain. Constraints on spatial variability of the regional geothermal heat flux in northern in Chile have been quantified by Hamza and Muñoz 1996 and Giese (1994), which suggest that subduction processes result in a steadily increasing heat flux of ~40 mW/m^2 at the Chilean coast (transect location A) to ~90 mW/m^2 beneath the Altiplano (transect location A′). As a result, the basal heat flux specified here increases linearly from 40 mW/m^2 at the Chilen coast to 90 mW/m^2 at the Chile-Bolivia border (Fig. 3).

Initial conditions were computed by simulating groundwater and heat flow within the model domain until gravity and thermal equilibrium were reached. Results of this simulation indicate that the spatially variable basal heat flux results in a steadily increasing steady-state geothermal gradient from 18 °C/km at the western boundary to 31 °C/km at the eastern boundary (Fig. 5). Additionally, these results indicate that the steady-state groundwater flow regime comprises three distinct features, which include (1) subbasin-scale groundwater circulation below Salar de Huasco; (2) rapid lateral groundwater flow from east-to-west within the Precordillera, and (3) upwelling below the PdT Basin.

Prioir to transient simulations, the model domain is augmented to include source terms for simulating the effects of meteoric water infiltration within the high elevation Altiplano. The source terms are parameterized on the basis of a high elevation groundwater recharge model developed for arid Andean aquifers by Houston (2006), which suggests that annual meteoric water infiltration (R, in mm) is a function mean annual precipitation (MAR), as given by

$$R = (0.44 \times \mathrm{MAR}) - 52.5 \quad (1)$$

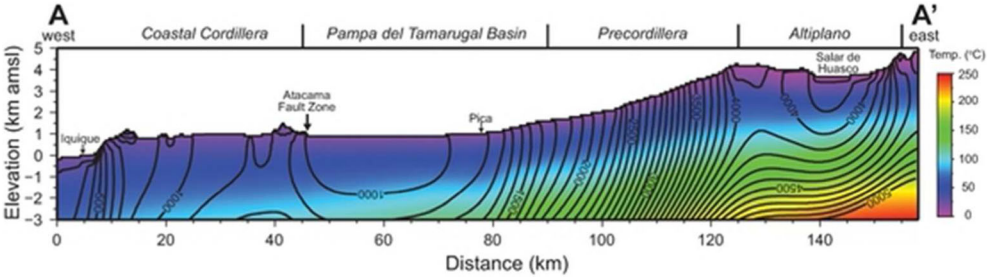

Fig. 5 Initial conditions for the groundwater and heat flow model across study area transect A–A′. The *color palette* is the initial temperature distribution and the *black contour lines* are hydraulic head at 100-m intervals

where MAR is quantified by Houston 2002 as,

$$\mathrm{MAR} = e^{\frac{A}{833}} \tag{2}$$

In Eq. (2), e is the natural exponential function, and A is elevation in m amsl. This expression for MAR indicates that annual precipitation in northern Chile decays exponentially with decreasing elevation (A). The spatial distribution of R is plotted as a function of elevation in Fig. 3 (inset), indicating that groundwater recharge within the study area transect is nil for elevations below 3,984 m amsl. In order to obviate the complexity associated with mixed-type boundary conditions, the infiltration cells are placed immediately below the surface boundary (Fig. 3), in accordance the approach adopted by Pollyea et al. 2015 for simulating infiltrating groundwater at the basin scale. In this approach, infiltrating meteoric water is inhibited from migrating upwards into the boundary cells by augmenting the model grid to change the connection distance between the center of each infiltration cell and its downward interface from 50 m to an infinitesimally small value, which

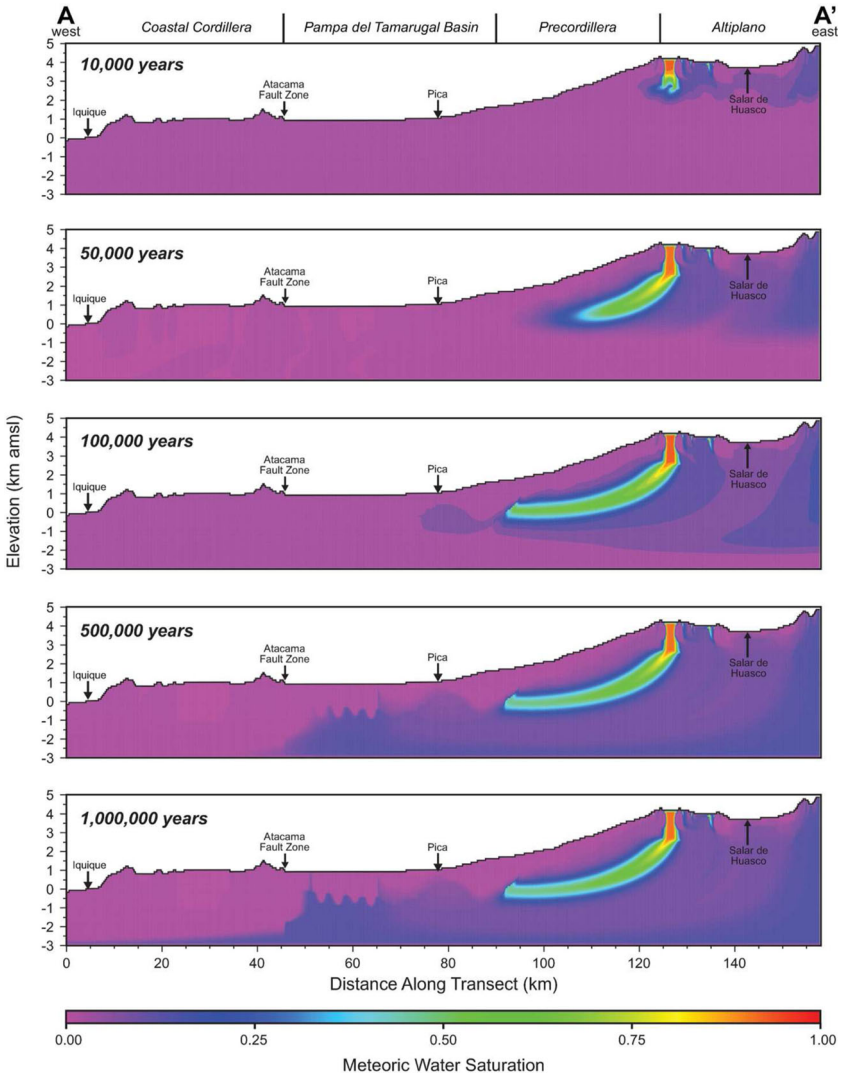

Fig. 6 Temporal progression of meteoric water infiltration and migration through the study area transect through 1 million years of simulation time. *Color palette* denotes saturation of meteoric water, which is nil for the initial water mass. Little change in this distribution occurs after 1 million years of simulation time, suggesting that the groundwater flow regime reaches steady state by this time

effectively places the infiltrating meteoric water at the interface between the source cell and its underlying neighbor. For transient simulations, the two-waters function of TOUGH2-MP/EOS1 (Zhang et al. 2008; Pruess et al. 1999) is invoked so that the saturation of infiltrating (meteoric) water and initial water are separately tracked through the model domain. In the two-waters formulation, individual mass balances are solved for each water component, while maintaining identical thermophysical water properties within each cell.

Parameter selection and analysis

In the closing discussion on numerical model development, a brief mention of parameter selection and the resulting uncertainty is warranted. A detailed literature review revealed little publicly available data for the thermal and hydraulic rock properties needed to parameterize the geologic formations within the study area. As a result, the geologic formations illustrated in Fig. 4 are parameterized with thermal and hydraulic properties on the basis of field and laboratory analyses for corresponding rock types, and these values are presented in Table 1. In order to evaluate the effects of this uncertainty on the regional-scale groundwater flow system, a parameter study found that regional flow paths are strongly influenced by the degree of permeability anisotropy in the crystalline basement rock. Field investigations of deep (6–9 km depth) crustal rocks have shown that in situ permeability varies over three orders of magnitude from ~10^{-18} to ~10^{-16} m^2 (Huenges et al. 1997). In accordance with these findings, the permeability model utilized for crystalline basement rocks in this study is characterized by an anisotropic permeability structure such that vertical permeability (k_v) is 9.87×10^{-18} m^2 and horizontal permeability (k_h) is 9.87×10^{-16} m^2. This permeability model for the basement rock results in a groundwater flow regime that is highly compatible with the stable isotope results within the western Pampa del Tamarugal basin; results from a parametric analysis of basement permeability anisotropy are presented in Figures S1 and S2 of the electronic supplementary material (ESM). Figure S1 of the ESM illustrates meteoric water saturation after 1 million years of simulation when vertical permeability is held constant at 9.87×10^{-18} m^2 and horizontal permeability varies from 9.87×10^{-18} m^2 to 9.87×10^{-15} m^2. Similarly, Figure S2 of the ESM illustrates groundwater residence time distribution after 1 million years of simulation when vertical permeability is held constant at 9.87×10^{-18} m^2 and horizontal permeability varies from 9.87×10^{-18} m^2 to 9.87×10^{-15} m^2.

Results

The numerical model simulates groundwater flow across the transect for 30 million years on the basis of numerous investigations suggesting that climate in the Atacama Desert has been stable for 16–25 million years (Alpers and Brimhall 1988; Garreaud et al. 2010; Hartley et al. 2005; Houston 2005; Rech et al. 2006; Sillitoe and McKee 1996). Results suggest that steady state is reached by 1 million years of simulation time, which will be used as the terminal time step for the following discussion. Figure 6 presents the temporal evolution of infiltrating meteoric water from the Altiplano to the Pampa del Tamarugal (PdT) basin. Figures 7 and 8 illustrate groundwater flux within the PdT basin (45–90 m along transect) and Salar de Huasco (125–158 m along the transect), respectively. The simulated groundwater residence time distribution is shown in Fig. 9. Oxygen isotope values measured in groundwater samples collected for this study range from –14.33 ‰ in groundwater samples from Salar de Huasco to +6.90 ‰ in Salar de Llamara. These data are presented in Table 2, and a summary of regional oxygen isotope variation is presented in Table 3. All oxygen isotope data used for the regional summary are included in Table S1 of the ESM.

Discussion

The implications of the numerical model and oxygen isotope results presented in the previous section are discussed in the following in the context of regional groundwater flow, and in the context of the spatial and temporal variations in meteoric water distributions. In addition, simulated groundwater residence time is discussed within the context of oxygen isotope values from both the field sampling campaign (Table 2) and regional averages compiled from the literature (Table 3). The final section presents interpretations of regional-scale groundwater flow in the context of the numerical model and oxygen isotope results.

Regional groundwater flow

Groundwater flow paths across the study area are reasonably explained by the pioneering works of Tóth (1962), which show that nested groundwater flow regimes arise when local-scale topographic variations are superimposed on a regional topographic gradient. Within the study area transect, the groundwater flow regime is governed by the combined effects of the high-elevation Altiplano subbasin and lower-elevation PdT Basin, which are separated by a steep topographic slope descending through the Precordillera. The regional hydraulic head gradient is east-to-west with a maximum lateral head gradient of 0.09 m/m in the Precordillera; however, this regional head gradient is locally interrupted in the east by the Altiplano, which is a high-elevation topographic depression bounded on the west by a subbasin drainage divide delineated by the Precordillera crest and on the east by the South American divide (Fig. 5). As a result, a portion

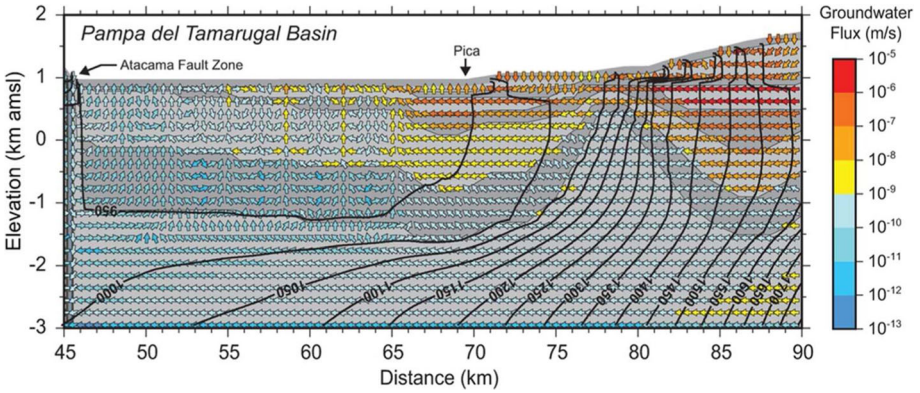

Fig. 7 Hydraulic head contours (*black lines*) at 50 m intervals and groundwater flux vectors are colored by magnitude at 1 million years of simulation time within the Pampa del Tamarugal Basin. Convection cells appear when head is less than 950 m due the combination of low head gradient and thermal buoyancy effects, which results in a physical mechanism for groundwater flow into the basin from depths beyond 2 km. Underlying geology is illustrated as alternating gray scale layers; see Fig. 4 for geological descriptions

of the meteoric water infiltrating within the Altiplano flows eastward towards Salar del Huasco. Within the central and western PdT Basin, the relatively flat topography results in a rapidly decreasing lateral head gradient from east to west, particularly at shallow depths. The flow paths and residence time distribution associated with this fluid system architecture are discussed in detail in the subsequent sections.

Meteoric water infiltration and flow paths

On the basis of Eqs. (1) and (2), groundwater infiltration occurs above 3,984-m elevation with annual infiltration rates ranging from 0.04 to ~100 mm (Fig. 5, inset). Calculated infiltration rates are in agreement with a published long-term average recharge of 22 mm/yr in the Salar de Huasco basin (Uribe et al. 2015). This infiltration occurs across two contiguous sections separated by the Salar de Huasco within which there is no infiltration due to low precipitation and high evaporative potential. The recharge zones comprise (1) a relatively flat, 15 km-wide topographic high marking the boundary between the Precordillera and Altiplano, and (2) a steep topographic slope bounding the Altiplano and terminating within the Andean Cordillera at the South American divide. In order to quantify the spatio-temporal evolution of this infiltration over geologic time, the meteoric water saturation is evaluated at discrete time-steps ranging from 10,000 to 1,000,000 years (Fig. 6).

At 10,000 years of simulation time, a subbasin-scale groundwater flow regime develops below Salar de Huasco (Fig. 6). This groundwater system is characterized by (1) downward infiltration from the bounding highlands to ~1 km depth, (2) topographically controlled lateral flow towards the salar, and (3) isolated upwelling within Salar de Huasco between 140 and 145 km along transect (Fig. 6). The spatial distribution of this upwelling comprises two mechanisms, which include near-surface flow from the eastern highlands and a deep contribution that appears isolated to the western portion of Salar de Huasco (Fig. 8). Near-surface flow paths in the eastern salar are geologically controlled by relatively high-permeability sedimentary units of the Altos de Pica formations (Fig. 4), which are present above a low-permeability clay unit, thus allowing rapid, shallow groundwater flow from the eastern highlands. The deep upwelling mechanism is a function of the higher infiltration rates and elevations within the Andean Cordillera. The combination of high infiltration rates and topographic potential increase the lateral head gradient below the eastern portion of the basin, thus driving groundwater farther west before the vertical head

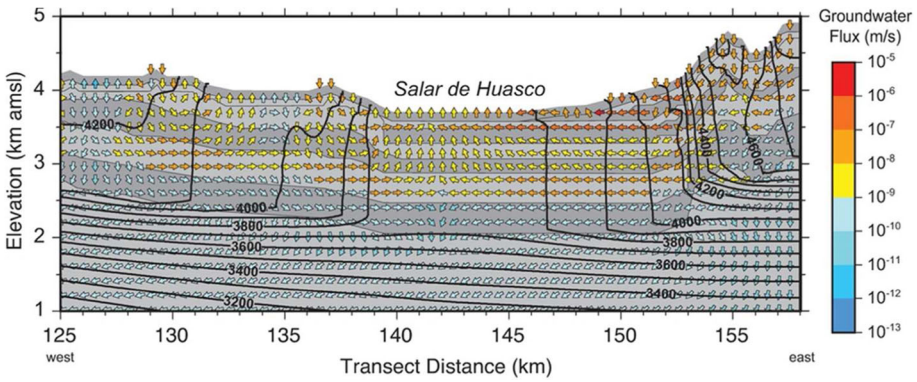

Fig. 8 Groundwater system within the Altiplano at 1 million years of simulation time. Hydraulic head contours (*black lines*) at 100-m intervals and groundwater flux vectors are colored by magnitude. Underlying geology is illustrated as alternating gray scale layers; see Fig. 4 for geological descriptions

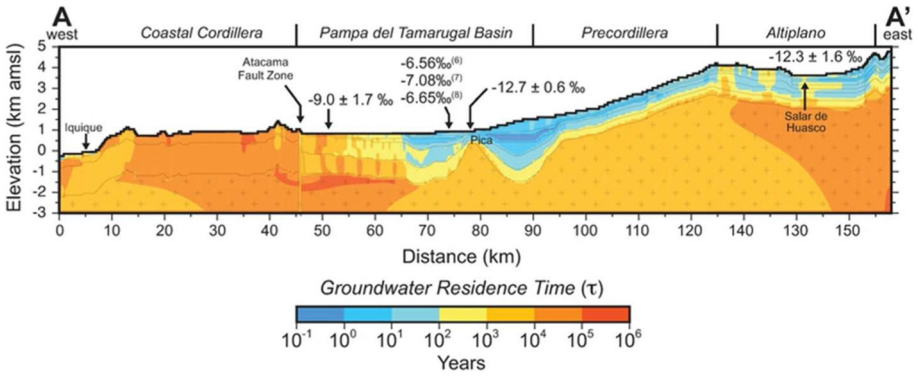

Fig 9 Contour plot of groundwater residence time with average regional $\delta^{18}O$ values measured in samples from shallow groundwater (wells) across the study area, in addition to three individual $\delta^{18}O$ values measured in samples from shallow groundwater wells ~5 km west of Pica. Sample locations for the individual samples are in parentheses and correspond with locations in Fig. 1. Regional $\delta^{18}O$ values in the western PdT, Pica, and Salar de Huasco are average values taken from the literature and samples analyzed for the present study (Tables 2 and 3, and Table S1 of the ESM)

gradient is strong enough to bring water upwards; however, this upwelling is inhibited by the presence of the laterally contiguous clay layer below Salar de Huasco (Fig. 8). As a result, upward flow from depth is isolated to a relatively small window between 141 and 142 km and ~3,500-m elevation. Although this process would likely be governed by structural discontinuities in the ignimbrite underlying Salar de Huasco, the general result is supported by field observations made in November 2014, as well as $\delta^{18}O$ values from this study and reported in the literature (Tables 2 and 3; Uribe et al. 2015), the latter of which are discussed in section 'Groundwater residence time and isotope geochemistry.' In particular, field observations found that Salar de Huasco presently comprises a groundwater fed lake on the western half of the basin along with several smaller springs on the margins.

In addition, the groundwater flow regime below Salar de Huasco at 10,000 years of simulation time suggests that a significant fraction of meteoric infiltration is reaching depths >2 km below the Precordillera-Altiplano boundary (Fig. 6). This vertical flow is driven by the subbasin drainage divide, which suppresses the influence of the regional head gradient causing a substantial portion of the meteoric water infiltration to flow vertically downward through the overlying marine sediments (Longacho and Cerro Empaxa Fms.) and into the underlying crystalline basement rock before westward migration under the influence of the regional east-to-west head gradient.

By 50,000 years of simulation time, the groundwater flow regime below Salar de Huasco is unchanged from the 10,000-year simulation, suggesting that steady state has been achieved within Salar de Huasco by 10,000 years. However, the 50,000 year time step suggests the regional east-to-west head gradient has captured the vertically penetrating meteoric water below the Precordillera-Altiplano boundary, as well as a proportion of infiltration along the South American drainage divide; and as a result, a large plume of groundwater with meteoric origin is migrating through the Precordillera within crystalline basement rock (Fig. 6). This process continues developing through 100,000 years, by which time the deeply penetrating groundwater from the South American divide has migrated upwards and merged with the large plume originating in the Altiplano. In addition, the leading edge of the meteoric water plume has reached the western Pampa del Tamarugal (PdT) Basin near the transect location demarcated by the town of Pica, Chile (77 km along transect). Interestingly, the combination of geological heterogeneity and flattening topographic gradient in this region interrupt the flow regime as the meteoric water plume leaves the deep, low-permeability Longacho shale formation ($k = 9.9 \times 10^{-16}$ m^2) and enters the high-permeability Cerro Empaxa sandstone formation ($k = 5.3 \times 10^{-14}$ m^2). Consequently, the Longacho Fm. governs the transport of meteoric water into the Cerro Empaxa formation, which ultimately follows the fold limb downward before migrating upwards into the Pica region (Fig. 7). This pattern is consistent through the remaining timesteps suggesting that the Longacho formation restricts groundwater circulation from the Altiplano into the PdT Basin; however, several warm springs are known to exist in the Pica region (Risacher et al. 2011) and are likely the result of a known, but poorly constrained fault system (Dingman and Galli 1965). Nevertheless, the Longacho formation is laterally continuous through the study area, and these results indicate that it may exert significant control on the timing of deep-seated groundwater recharge into the PdT Basin.

After 500,000 years of simulation time, the infiltrating meteoric water has reached the full lateral extent of the PdT Basin, and the system reaches a steady state by 1,000,000 years (Fig. 6). Within the PdT Basin, two distinct features characterize the groundwater flow system. In the eastern half of the basin, the regional head gradient associated with the Precordillera drives horizontal flow westward with decreasing flux magnitude as the topographic gradient

Table 2 Oxygen isotope values collected and analyzed for this study

Figure 1 location	Sample type	Location/sample ID	Elevation (m amsl)	Coordinates (UTM WGS84 19 K)		$\delta^{18}O$ (‰ VSMOW)
1	Spring	Iquique, Costal Spring (CS14-01)	35	379235	7740032	–7.37
2	Groundwater	La Tirana Well (LL14-07)	766	435497	7647839	–7.10
3	Groundwater	Cuminalla Well (C13-04)	996	434217	7743784	–9.90
4	Groundwater	Cuminalla Well (C13-06)	996	434167	7743843	–10.15
5	Groundwater	Cuminalla well (C14-10)	996	434217	7743784	–9.69
6	Groundwater	La Calera Well (LC14-05)	1,109	455167	7745880	–6.56
7	Groundwater	La Calera Well (LC14-04)	1,109	455167	7745880	–7.08
8	Groundwater	La Calera Well (LC14-01)	1,389	458926	7748123	–6.65
9	Spring	Pica (P14-01)	1,391	466944	7734743	–12.45
10	Spring	Pica (P14-02)	1,391	466944	7734743	–13.05
11	Spring	Pica (P14-03)	1,391	466944	7734743	–13.12
12	Spring	Pica (P14-05)	1,391	466944	7734743	–13.01
13	Spring	Quisma (Q12-01)	1,395	466942	7739323	–13.24
14	Spring	Quisma (Q13-01)	1,395	466952	7734761	–13.30
15	Spring	Quisma (Q14-01)	1,283	464268	7731614	–12.93
16	Groundwater	Quisma Canyon (Q12-02)	1,274	463976	7731102	–12.80
17	Groundwater	Pica Well (P13-01)	1,485	469750	7731265	–12.20
18	Groundwater	Pica Well (P12-02)	1,485	469507	7731226	–11.17
19	Groundwater	Salar de Huasco Well (HAS14-08B)	3,954	517996	7784042	–14.33
20	Groundwater	Salar de Huasco Well (HAS14-02A)	3,791	512439	7753565	–11.99
21	Spring	Salar de Huasco (HAS14-01)	3,784	511514	7757229	–12.23
22	Spring	Salar de Huasco (HAS14-07A)	3,794	512951	7759471	–11.96
23	Spring	Salar de Huasco (HAS14-07B)	3,794	512951	7759471	–12.00
25	Salar	Salar de Llamara (LL12-09a)	754	433951	7647851	5.63
26	Salar	Salar de Llamara (LL12-09b)	754	433951	7647851	5.80
27	Salar	Salar de Llamara (LL12-16)	754	435943	7648160	6.09
28	Salar	Salar de Llamara (LL13-02)	754	435962	7648081	6.90
29	Salar	Salar de Llamara (LL13-16)	754	434646	7648407	6.50
30	Salar	Salar de Llamara (LL13-17)	754	433944	7647852	6.70

The $\delta^{18}O$ values of water samples were measured at the Northern Illinois University stable isotope laboratories via CO_2 equilibration on a GasBench II coupled to a Thermo MAT253 isotope ratio mass spectrometer in continuous flow. $\delta^{18}O$ values are reported in VSMOW with an analytical precision of ±0.3 ‰

flattens. Within the western half of the basin, the Atacama Fault Zone inhibits westward groundwater flow due to the low-permeability fault core, which in combination with the broad, flat topography results in a substantially lower head gradient that permits thermally driven convection cells to develop (Fig. 7). Although the spatial orientation of these convection cells may arise from model grid discretization, this result suggests that the low topographic driving potential combined with sufficient basal heat flux permits the upward migration of relatively deep groundwater in this region.

The flow paths transporting groundwater of meteoric origin to shallow aquifers within the western PdT Basin are evident as mounds of elevated meteoric water saturation between 50 and 67 km along transect after 1 M years of simulation time (Fig. 6). This deep-seated upward circulation begins in the east at ~67 km along the transect where the high-permeability Cerro Empaxa sandstone folds sharply upwards as the regional topographic gradient subsides (Fig. 7). The western extent of this recharge zone occurs at ~51 km along transect in response to the Atacama Fault Zone, which inhibits westward groundwater flow. In this region, vertical head gradients are favored to near-surface depths because the high-permeability Altos de Pica 3 sandstone pinches out, which leaves lower-permeability formations juxtaposed with the

Table 3 Summary of regional oxygen isotope values of water in the study area. Note: For $\delta^{18}O$, average values are reported in per mil (‰) relative to VSMOW. The standard deviation (2σ) and number of samples (n) are also reported

Location	Sample type	Elevation (m amsl)	$\delta^{18}O$	(2σ)	n	Sample year(s)	Sources
N. Chile	Precipitation	<3,000	–5.9	3.2	25	1973–2013	a,b,c,e
		3,000–4,000	–12.8	5.9	68	1973–2013	
		>4,000	–15.0	6.1	69	1973–2013	
Salar de Huasco	Groundwater	3,873 ± 115	–12.3	1.6	13	2008–2014	d,e
	Surface water	3,917 ± 139	–12.2	1.3	10	1997–2014	d,e
	Spring	4,003 ± 321	–13.1	1.1	14	2009–2014	d,e
	Precipitation	4,249 ± 316	–15.6	2.7	9	2010–2011	e
Pica	Groundwater and springs	1,351 ± 137	–12.7	0.6	11	2011–2014	a,d,e
PdT Basin	Groundwater	1,203 ± 161	–9.0	1.7	27	1972–2014	a,d
Salar de Llamara	Salar	754 ± 1	+6.3	0.5	6	2012–2014	d

[a] Fritz et al. (1981)

[b] Alpers and Whittemore (1990)

[c] IAEA/WMO (2014)

[d] This study

[e] Uribe et al. (2015)

The complete dataset used for preparing this summary table is presented in Table S1 of the electronic supplementary material (ESM)

unconsolidated cover. Interestingly, salars within the PdT Basin occur exclusively along the western extent (Fig. 1), and these modeling results provide a theoretical basis for this phenomenon. In addition, Magaritz et al. 1990 hypothesized that deep, hydrothermal groundwater circulation into the PdT Basin likely results from a deep fracture network underlying the sedimentary cover. The modeling results presented here suggest that such flow paths are not dependent on a deep fracture network; however, the presence of a deep-seated fracture system would likely increase the contribution of upward flow.

Although the model domain continues west towards the Pacific Coast, the authors believe that interpretations beyond the Atacama Fault Zone are unreliable due to poor geological constraints on the Atacama Fault Zone. As a result, this portion of the model domain is used primarily to mitigate non-physical boundary effects from influencing the simulation results, and caution is warranted in making inferences west of ~45 km along the transect.

Groundwater residence time and isotope geochemistry

Groundwater residence time is an important criterion for understanding the temporal variability of groundwater recharge across regional terrains (e.g., Jiang et al. 2010). In order to quantify the groundwater residence time (τ) distribution across the study area transect, τ is computed within each grid cell using the traditional formulation: $\tau = V_w/Q$, where V_w (m^3) is the volume of groundwater (grid cell volume × porosity) in each cell and Q (m^3/s) is the net volumetric flow rate through each cell, which is computed with TOUGH2-MP output as net mass flux (kg/s) divided by water density (kg/m^3). The groundwater residence time distribution is shown in Fig. 9, which indicates that τ varies over 6 orders of magnitude, ranging from 10^0 years to $>10^5$ years. As would be expected, groundwater residence generally increases with depth and decreases with increasing topographic slope; however, several exceptions are observed within Salar de Huasco and the Pampa del Tamarugal (PdT) Basin.

The groundwater flow regime within Salar de Huasco is characterized by a residence time distribution ranging between 10^0 and 10^3 years, in which low τ waters are present at shallow depths and comparatively high τ groundwater occurs within and below the low-permeability clay layer underlying the salar (Fig. 9). Historically, regional-scale variations of oxygen and hydrogen isotope values for various water reservoirs in the PdT (e.g. meteoric, surface water, groundwater) have provided the framework for interpreting hydrologic variations (e.g. Fritz et al. 1981; Aravena et al. 1999). Consequently, the model results of this study are discussed in the context of $\delta^{18}O$ variations in both newly collected water samples and values reported in the literature. Regional-scale variations in the relationship between δ^2H and $\delta^{18}O$ values of waters have been reported extensively in the literature; therefore, only the $\delta^{18}O$ values are reported here for simplicity. A more detailed examination of the isotope variations in regional waters may be warranted, but is outside the scope of this study; nevertheless, the regional variation of $\delta^{18}O$ values measured in waters collected for this study range from –14.33 ‰ in Salar de Huasco to +6.9 ‰ in Salar Llamara (Table 2), which is in general agreement with regional averages reported in the literature (Table 3 and Table S1 of the ESM).

In northern Chile, $\delta^{18}O$ values in precipitation decrease by as much as 0.64 ‰ per 100 m of elevation gain as air masses move into the higher elevations of the Andes, the result of which is a regional altitudinal gradient in the $\delta^{18}O$ values of precipitation. Consequently, the observed variability in surface water in the Salar de Huasco basin likely reflects the combination of altitude effects on the $\delta^{18}O$ values of precipitation and extreme evaporation on the $\delta^{18}O$ values in the surface waters of the Salar de Huasco (Uribe et al. 2015; Aravena et al. 1999). The mean $\delta^{18}O$ values measured in precipitation from samples collected in a two-year study (2010–2011) at Salar de Huasco are reported as -15.6 ± 2.7 ‰ (Uribe et al. 2015), while mean $\delta^{18}O$ values measured in groundwater and surface water (the salar lake) within Salar de Huasco are reported as -12.3 ± 1.6 and -12.2 ± 1.3 ‰, respectively (Table 3). Consequently, groundwater reservoirs within Salar de Huasco comprise slightly higher $\delta^{18}O$ values than average precipitation or seasonal springs with very small τ in the Salar de Huasco Basin (Ave. $\delta^{18}O = -13.1 \pm 1.1$ ‰; Table 3). Although this investigation does not purport to decipher the complete geochemical signal of these groundwater-fed salars, increases of a few ‰ in $\delta^{18}O$ values resulting from evaporative processes (at ground surface and within the vadose zone) is in general agreement with the numerical modeling results, which indicate relatively rapid groundwater cycling from the high elevation recharge areas bounding the arid Salar de Huasco.

Within the Precordillera, the groundwater residence time ranges between 10^0 and 10^2 years within the upper km of the model domain (Fig. 9). These relatively small τ values arise due to the high-permeability sedimentary units overlying the low-permeability crystalline basement, which in combination with the high head gradient in this region results in rapid groundwater flux through the sedimentary cover. This effect is particularly pronounced below the boundary separating the Precordillera and PdT Basin, where τ is on the order of 10^0 years at 500–750 m depth within the Altos de Pica 5 sandstone ($k = 5.3 \times 10^{-13}$ m^2). This τ distribution is consistent through the eastern third of the PdT Basin, where the regional east-to-west head gradient governs the groundwater system; however, the $\delta^{18}O$ values from spring water samples collected near Pica suggests a more complex hydrogeological framework. In particular, there are two distinct groups of water samples from (1) groundwater and springs near Pica ($\delta^{18}O = -12.7 \pm 0.6$ ‰) and (2) three groundwater samples (6, 7, 8 in Table 2) from wells in the PdT ~5 km west of Pica with $\delta^{18}O$ values of –6.56,–7.08, and –6.65 ‰ (Fig. 9). On the basis of low residence time and high head gradient immediately east of Pica, the modeling results rule out a high likelihood of strong evaporative enrichment or water–rock interaction in the waters at Pica. This result is in agreement with low $\delta^{18}O$ values measured at Pica that are nearly identical to the groundwater $\delta^{18}O$ values from the high elevation source areas in Salar de Huasco. The combination of low $\delta^{18}O$ values and low simulated residence times are suggestive of a meteoric source with rapid subsurface flow paths, which is in general agreement with the Houston (2002) recharge hypothesis that suggests periodic storm events in the Altiplano recharge aquifers in the PdT basin through near-surface alluvial fan drainage. However, this near-surface recharge mechanism is likely limited to aquifers within the eastern basin on the basis of the rapidly decreasing head gradient within the eastern portion of the PdT, which would inhibit the development of near-surface flow paths across the lateral extent of the basin. Moreover, this recharge mechanism does not explain the substantially higher $\delta^{18}O$ values measured in samples ~5 km west of Pica (Fig. 9), which are suggestive of strong evaporative enrichment or water–rock interactions. The modeling results suggest that these comparatively higher $\delta^{18}O$ values are likely a result of water–rock interactions, and it is hypothesized that a poorly constrained fault system underlying Pica (Dingman and Galli 1965) is a likely source for hydrothermally altered groundwater. This fault system is not simulated here due to unknown spatial and parametric constraints; however, upwardly folded basement rocks occur at depths < 1 km, which is a potential source for hydrothermally altered fluids to reach shallow depths and discharge within the shallow groundwater system near Pica.

Within the western PdT Basin (45–65 km along transect), groundwater residence time ranges from 10^3 to 10^5 years (Fig. 9), which is substantially longer than in the eastern basin, and suggests a minimal influence of shallow recharge mechanisms from near-surface flow coming off the Precordillera. The elevated $\delta^{18}O$ values (Ave. +3.7 ‰ relative to Pica) observed in groundwater collected in the western PdT Basin indicate the waters are out of equilibrium with meteoric $\delta^{18}O$ values in high altitude recharge areas, suggesting (1) the measured $\delta^{18}O$ values may be the result of both evaporative processes and fluid–rock interactions at depth, or (2) groundwater in the western PdT represents temporal variation in the $\delta^{18}O$ values of infiltrating meteoric water (e.g., increased precipitation at lower elevations in the PdT basin) not seen in the modern dataset (e.g. Aravena et al. 1999). The evaporation potential within the PdT Basin is extreme, and groundwater fed salars along its western extent are characterized by highly brackish water with abundant evaporative mineral deposits covering large areal extents and extremely high $\delta^{18}O$ values (e.g. $+6.3 \pm 0.5$ ‰ in Salar de Llamara; Fig. 1). However, the numerical model results also provide a theoretical basis for groundwater originating in the Altiplano to recharge shallow aquifers and salars in the western PdT Basin through deep groundwater circulation in crystalline basement rocks, which can also result in the +3.7 ‰ increase in $\delta^{18}O$ values PdT groundwater from the meteoric source. This recharge mechanism is shown to operate on a time scale of 10^5 years, and includes vertical meteoric water infiltration

to depths >2 km below the Altiplano followed by westward migration within the Precordillera through crystalline basement rocks before discharging within the western PdT Basin (Fig. 6). It is impossible to conclusively rule out temporal variation in the source region or hydrothermal alteration as the cause of elevated $\delta^{18}O$ values of groundwater in the western PdT Basin; however, both processes are in agreement with the recharge time scale of 10^5 years.

Integrated model and stable isotope interpretations

Results from this study show that Salar de Huasco (a high elevation topographic depression) creates a local drainage divide below the Precordillera-Altiplano boundary, which permits infiltrating groundwater to reach depths in excess of 2 km depth before westward migration through the crystalline basement rocks. As the infiltrating meteoric water reaches the eastern PdT Basin, upward migration is inhibited by the low-permeability Longacho formation, which folds upwards below the Pica region creating a bottleneck and locally increasing the head gradient below Pica. In this region, the $\delta^{18}O$ variation in spring water samples is complex, and suggests the presence of groundwater with both meteoric and hydrothermal sources that may be the result of (1) deep groundwater upwelling through a poorly constrained fault system near Pica, and (2) near-surface groundwater flow originating as periodic floodwaters at high elevation. This latter inference is in agreement with the Houston (2002) recharge model. Groundwater flow within western PdT Basin is governed by the presence of the Atacama Fault Zone, which is characterized by a low-permeability fault core that inhibits across-strike flow. As a result, the regional east–west head gradient is fully suppressed west of ~65 km along the transect and at depths above 2 km. Consequently, the groundwater flow regime in this region is governed by thermal effects, which manifest in the model results as convection cells between 50 and 65 km along the transect. Although the spatial distribution of these convection cells may be a result of grid size, their presence in the simulation results suggests that deep, hydrothermal circulation is likely occurring in the western PdT Basin on time-scales of 10^4–10^5 years. Moreover, the upwelling associated with this process is localized in the western portion of the basin, providing a mechanism and time scale for the source and formation of salars within the PdT Basin. This result is in general agreement with the aquifer recharge model proposed by Magaritz et al. 1990, which argued for a thermally driven basal aquifer recharge flux through deep-seated basin fractures.

The combined model and isotopic results suggest that both previously proposed aquifer recharge mechanisms (Houston 2002; Magaritz et al. 1990 are likely influencing aquifers within the PdT Basin; however, each mechanism is operating on different spatial and temporal scales. In particular, this study finds that storm-driven flood events in the Altiplano would readily transmit groundwater to the eastern PdT Basin through near-surface groundwater flow on short time scales, e.g., 10^0–10^1 years. However, these effects would likely be isolated to aquifers in the eastern third of the basin because the regional head gradient drops rapidly west of Pica. In addition, these results also provide a physically plausible mechanism for groundwater originating in the eastern highlands to reach the PdT Basin; however, this mechanism is operating on a timescale of 10^4–10^5 years and is localized to the western half of the basin, where the lateral head gradient is suppressed by the presence of the Atacama Fault Zone, thus permitting thermal effects to drive groundwater upwards.

Conclusions

This paper presents results of a regional-scale groundwater investigation at ~20.5°S latitude in northern Chile. This study is designed to enhance our understanding of regional-scale groundwater flow from high-elevation recharge areas in the Andean Altiplano into aquifers within the Pampa del Tamarugal (PdT) Basin. Although it is widely accepted that aquifer recharge in the PdT Basin originates as precipitation in the Altiplano and Andean Cordillera to the east, there remains debate on whether the aquifer recharge results primarily from deep groundwater circulation (Magaritz et al. 1990 or storm-driven flood events (Houston 2002). In order to fill this gap in knowledge, this study combines a regional-scale 2-D numerical model of heat and groundwater flow with $\delta^{18}O$ values measured in samples obtained along a study area transect to develop a quantitative conceptual model of groundwater flow at 20.5°S latitude across northern Chile. Results from this study show that both previously proposed aquifer recharge mechanisms are likely recharging aquifers within the PdT Basin; however, each mechanism is operating on different spatial and temporal scales. These results suggest that storm-driven flood events may transmit groundwater to the eastern PdT Basin on time scales of 10^0–10^1 years, while deep groundwater circulation is recharging PdT aquifers in the western basin on time scales of 10^4–10^5. This study may have important implications for regional groundwater resource management because PdT aquifers are the sole source of municipal water for the coastal City of Iquique (population ~215,000), as well as the economically important mining industry. In addition, these results provide important constraints on groundwater resource availability over time scales of interest for researchers seeking inputs on Holocene groundwater availability.

Acknowledgements This project received support from the National Geographic Society Waitt Grant No. W292-13 (Dodd), the Geological Society of America Graduate Student Research Grant (Jayne), the

Goldich Fund administered by the NIU Department of Geology and Environmental Geosciences (Jayne), the NIU College of Liberal Arts and Sciences (Dodd and Pollyea), and Beloit College (Swanson). The authors extend sincere thanks to associate editor William Anderson, Jr. and to Sara Taviani, Charles Heywood, and one anonymous reviewer for their insightful review comments, which dramatically improved the quality of the manuscript.

References

Acosta O, Custodio E (2008) Impactos ambientales de las extracciones de agua subterranean en el Salar del Huasco (norte de Chile) [Environmental impacts of groundwater withdrawals in the Salar del Huasco (northern Chile)]. Bol Geol Min 119(1):33–50

Alpers C, Brimhall GH (1998) Middle Miocene climatic change in the Atacama Desert, northern Chile: evidence from supergene mineralization at La Escondida. Geol Soc Am Bull 100:1640–1656

Alpers C, Whittemore D (1990) Hydrogeochemistry and stable isotopes of groundwater and surface waters from two adjacent closed basins, Atacama Desert, northern Chile. Appl Geochem 5:719–734

Amundson R, Dietrich W, Bellugi D, Ewing S, Nishiizume K, Chong G, Owen J, Finkel R, Heimsath A, Steward B, Caffee M (2012) Geomorphic evidence for the late Pliocene onset of hyperaridity in the Atacama Desert. GSA Bull 124(7/8):1040–1070. doi:10.1130/B30445.1

Aravena R, Suzuki O, Pena H, Pollastri A, Fuenzalida H, Grilli A (1999) Isotopic composition and origin of the precipitation in northern Chile. Appl Geochem 14(4):411–422. doi:10.1016/S0883-2927

Bacon C (1975) High-temperature heat capacity of silicate glasses. PhD Thesis, University of California, Berkeley, CA

Brace W (1980) Permeability of crystalline and argillaceous rocks. Int J Rock Mech Mining Sci Geomech Abstracts 17(5)

Cembrano J, González G, Arancibia G, Ahumada I, Olivares V, Herrea V (2005) Fault zone development and strain partitioning in an extensional strike-slip duplex: a case study from the Mesozoic Atacama fault system, northern Chile. Tectonophysics 400:105–125

Clarke J (2006) Antiquity of aridity in the Chilean Atacama Desert. Geomorphology 73(1–2):101–114. doi:10.1016/j.geomorph.2005.06.008

Daly R, Manger G, Clark S (1966) Section 4: density of rocks. GSA Memoirs, 97, GSA, Boulder, CO, pp 19–26

Dingman RJ, Galli CO (1965) Geology and ground-water resources of the Pica area, Tarapaca Province, Chile. No. 1189, US Gov. Printing Office, Washington, DC

Dorador C, Via I, Remonsellez F, Imhoff J, Witzel K (2010) Unique clusters of Archaea in Salar de Huasco: an athalassohaline evaporitic basin of the Chilean Altiplano. FEMS Microbiol Ecol 73:291–302

Eppelbaum LV, Kutasov I, Pichin A (2014) Applied geothermics. Springer, Heidelberg, Germany

Evans JP, Forster CB, Goddard JV (1997) Permeability of fault-related rocks, and implications for hydraulic structure of fault zones. J Struct Geol 19:1393–1404

Farías M, Charrier R, Comte D, Martinod J, Herail D (2005) Late Cenozoic deformation and uplift of the western flank of the Altiplano: evidence from the depositional, tectonic, and geomorphologic evolution and shallow seismic activity (northern Chile at 19 degrees 30′ S). Tectonics 24(4)

Farquharson J, Heap M, Varey N, Baud P, Reuschlé T (2015) Permeability and porosity relationships of edifice-forming andesites: a combined field and laboratory study. J Volcanol Geotherm Res 297:52–68

Fetter C (2001) Applied hydrogeology. Prentice Hall, Englewood Cliffs, NJ

Fitts C (2013) Groundwater science. Academic, Oxford

Forster C, Smith L (1998) Groundwater flow systems in mountainous terrain, 1: numerical modeling technique. Water Resour Res 24(7):999–1010

Fritz P, Suzuki O, Silvia C, Salati E (1981) Isotope hydrology of groundwater in the Pampa del Tamarugal, Chile. J Hydrol 53(1–2):161–184. doi:10.1016/0022-1694

Garizone C, Hoke G, Libarkin J, Withers S, MacFadden B, Eiler J, Ghosh P, Mulch A (2008) Rise of the Andes. Science 320(5881):1304–1307

Garreaud RD, Molina A, Farias M (2010) Andean uplift, ocean cooling and Atacama hyperaridity: a climate modeling perspective. Earth Planet Sci Lett 292:39–50

Gayo EM, Latorre C, Jorder TE, Nester PL, Estay SA, Ojeda KF, Santoro CM (2012) Late Quaternary hydrological and ecological changes in the hyperarid core of the northern Atacama Desert (similar to 21 degrees S). Earth Sci Rev 113(3–4):120–140. doi:10.1016/j.earscirev.2012.04.003

Ge S, Garven G (1989) Tectonically induced transient groundwater flow in foreland basin. In: Price RA (ed) The origin and evolution of sedimentary basins and their energy and mineral resources. Am Geophys Union Geophys Monog 48:145–157. doi:10.1029/GM048p0145

Giese P (1994) Geothermal structure of the Central Andean Crust: implications for heat transport and rheology. In: Tectonics of the Southern Central Andes. Springer, Heidelberg, Germany, pp 69–76

Gregory-Wodzicki KM (2000) Uplift history of the Central and Northern Andes: a review. Geol Soc Am Bull 112(7):1091–1105

Hamza V, Muñoz M (1996) Heat flow map of South America. Geothermics 25(6):599. doi:10.1016/S0375-6505(96)00025-9

Hartley AJ, Evenstar L (2010) Ceonzoic stratigraphic development in the north Chilean forearc: implications for basin development and uplift history of the Central Andean margin. Tectonophysics 495:67–77

Hartley AJ, May G, Chong G, Turner P, Kape SJ, Jolley EJ (2000) Development of a continental forearc: a Cenozoic example from the Central Andes, northern Chile. Geology 28(4):321–324

Hartley AJ, Chong G, Houston J, Mather AE (2005) 150 million years of climatic stability: evidence from the Atacama Desert, northern Chile. J Geol Soc Lond 162:421–424

Hoke GD, Isacks BL, Jordan TE, Yu JS (2004) Groundwater-sapping origin for the giant quebradas of northern Chile. Geology 32(7):605–608. doi:10.1130/F20601.1

Horton G, Hampton B, LaReau B, Baldellón (2002) Tertiary provenance history of the northern and central Altiplano (central Andes, Bolivia): detrital record of plateau-margin tectonics. J Sediment Res 72:711–726

Houston J (2002) Groundwater recharge through an alluvial fan in the Atacama Desert, northern Chile: mechanisms, magnitudes and causes. Hydrol Process 16(15):3019–3035. doi:10.1002/hyp.1086

Houston J (2005) The great Atacama flood of 2001 and its implications for Andean hydrology. Hydrol Process 20:591–610

Houston J (2006) Variability of precipitation in the Atacama Desert: its causes and hydrological impact. Int J Climatol 26:2181–2198. doi:10.1002/joc.1359

Huenges E, Erzinger J, Kück J, Engeser B, Kessels W (1997) The permeable crust: geohydraulic properties down to 9101 m depth. J Geophys Res 102(B8):255–18,265

IAEA/WMO (2014) Global network of isotopes in precipitation, the GNIP Database. http://www.iaea.org/water. Accessed 15 January 2016

JICA-DGA-PCI (Japanese International Cooperation Agency, Dirección General de Aguas, Pacific Consultants International) (1995) The study on the development of Water Resources in northern Chile. Technical reports. Supporting reports B and C, Centro de Información de Recursos Hídricos, Dirección General de Aguas, Ministerio de Obras Públicas, Santiago, Chile

Jiang XW, Wan L, Cardenas BM, Ge S, Wang XS (2010) Simultaneous rejuvenation and aging of groundwater in basins due to depth-decaying hydraulic conductivity and porosity. Geophys Res Lett 37:L05403. doi:10.1029/2010GL042387

Johnson G, Olhoeft GG (1984) Density of rocks and minerals. CRC Handbook of Physical Properties of Rocks, vol 3. CRC, Boca Raton, FL

Kösters M, Götze HJ, Schmidt S, Fritsch J, Araneda M (1997) Gravity field of a continent-ocean transition mapped from land, air, and sea. Eos 78:13–16

Kramer W, Siebel W, Romer R, Günther H, Zimmer M, Ehrlichmann R (2005) Geochemical and isotopic characteristics and evolution of the Jurassic volcanic arc between Arica (18°30′S) and Tocopilla (22°S), North Chilean Coastal Cordillera. Chemie der Erde 65:47–78

Lamb S, Hoke L (1997) Origin of the high plateau in the Central Andes, Bolivia, South America. Tectonics 16(4):623–649

Loveless JP, Hoke GD, Allmendinger RW, Gonzalez BL, Carrizo DA (2005) Pervasive cracking of the northern Chilean Coastal Cordillera: new evidence for forearc extension. Geology 33(12): 973–976

Magaritz M, Aravena R, Peña H, Suzuki O, Grilli A (1989) Water chemistry and isotope study of streams and springs in northern Chile. J Hydrol 108:323–341

Magaritz M, Aravena R, Peña H, Suzuki O, Grilli A (1990) Source of groundwater in the deserts of northern Chile: evidence of deep circulation of groundwater from the Andes. Ground Water 28(4):513–517. doi:10.1111/j.1745-6584.1990.tb01706.x

Mpodozis C, Ramos V (1989) The Andes of Chile and Argentina. In: Eriksen G et al. (eds) Geology of the Central Andes and its relation to Hydrocarbon and Mineral Resources. Earth Sci Ser 11:59–90

Nester P (2008) Basin and paleoclimate evolution of the Pampa del Tamarugal forearc valley, Atacama Desert, northern Chile. PhD, Cornell University, Cornell, NY

Nester PL, Gayo E, Latorre C, Jordan TE, Blanco N (2007) Perennial stream discharge in the hyperarid Atacama Desert of northern Chile during the latest Pleistocene. Proc Natl Acad Sci USA 104(50): 19724–19729. doi:10.1073/pnas.0705373104

Nuñez J, Verbist K, Wallis J, Schaefer M, Morales L, Cornelis W (2011) Regional frequency analysis for mapping drought events in north-central Chile. J Hydrol 405:352–366. doi:10.1016/j.jhydrol.2011.05.035

Oyarzún J, Oyarzún R (2011) Sustainable development threats, inter-sector conflicts and environmental policy requirements in the arid, mining rich, Northern Chile Territory. Sustain Dev 19:263–273. doi:10.1002/sd.441

Pollyea RM, Van Dusen EW, Fischer MP (2015) Topographically driven fluid flow within orogenic wedges: effects of taper and depth-dependent permeability. Geosphere 11:1427–1437. doi:10.1130/GES01120.1

Pruess K, Oldenburg C, Moridis G (1999) TOUGH2 user's guide, version 2. Technical report, LGNL-43134. Lawrence Berkeley National Laboratory, Berkeley, CA

Rech JA, Currie BS, Shullenberger ED, Dunagan SP, Jordan TE, Blanco N, Tomlinson AJ, Rowe HD, Houston J (2010) Evidence for the development of the Andean rain shadow from a Neogene isotopic record in the Atacama Desert, Chile. Earth Planet Sci Lett 292:371–382. doi:10.1016/j.epsl.2010.02.004

Rech JA, Currie BS, Michalski G, Cowan AM (2006) Neogene climate change and uplift in the Atacama Desert, Chile. Geology 34(9):761–764

Risacher F, Alonso H, Salazar C (2003) The origin of brines and salts in Chilean salars: a hydrochemical review. Earth Sci Rev 63:249–293

Risacher F, Fritz B, Hauser A (2011) Origin of components in Chilean thermal waters. J S Am Earth Sci 31:153–170. doi:10.1016/j.sames.2010.07/002

Rojas R, Dassargues A (2007) Groundwater flow modelling of the regional aquifer of the Pampa del Tamarugal, northern Chile. Hydrogeol J 15(3):537–551. doi:10.1007/s10040-006-0084-6

Rojas R, Batelaan O, Feyen L, Dassargues A (2010) Assessment of conceptual model uncertainty for the regional aquifer Pampa del Tamarugal - North Chile. Hydrol Earth Syst Sci 14(2):171–192

Sharma D (1997) Reservoir characterization of Yates Formation (Permian, Guadalupian), South Ward Field, Ward County, Texas. PhD Thesis, Texas A & M University, College Station, TX

Sillitoe R, McKee E (1996) Age of supergene oxidation and enrichment in the Chilean porphyry copper province. Econ Geol 91(1):164–179

Smyth R, Sharp J (2006) The hydrology of tuffs. Geol Soc Am Spec Pap 408:91–111

Stoertz GE, Ericksen GE (1974) Geology of salars in northern Chile. US Geol Surv Prof. Paper 811

Tóth J (1962) A theory of groundwater motion in small drainage basins in central Alberta, Canada. J Geophys Res 67(11). doi: 10.1029/JZ067i011p04375

Tóth J (1963) A theoretical analysis of groundwater flow in small drainage basins. J Geophys Res 68(16). doi: 10.1029/JZ068i008p02354

Uribe J, Muñoz JF, Gironás R, Aguirre E, Aravena R (2015) Assessing groundwater recharge in an Andean closed basin using isotopic characterization and a rainfall-runoff model: Salar de Huasco basin, Chile. Hydrogeol J 23(7):1535–1551. doi:10.1007/s10040-015-1300-z

Valero-Garcés BL, Grosjean M, Kelts K, Shreier H, Messerili B (1999) Holocene lacustrine deposition in the Atacama Altiplano: facies models, climate and tectonic forcing. Palaeogeogr Palaeoclimatol Palaeoecol 151:101–125

Victor P, Oncken O, Glodny J (2004) Uplift of the western Altiplano plateau: evidence from the Precordillera between 20 degrees and 21 degrees S (northern Chile). Tectonics 23(4)

Wang J, Narasimhan T (1985) Hydrologic mechanisms governing fluid flow in a partially saturated, fractured, porous medium. Water Resour Res 21:1861–1874

Zhang K, Wu YS, Pruess K (2008) User's guide for TOUGH2-MP: a massively parallel version of the TOUGH2 Code. Technical report, LBNL-315E, Lawrence Berkeley National Laboratory, Berkeley, CA